# SUBGROUP IDENTIFICATION THROUGH MULTIPLEX COMMUNITY STRUCTURE WITHIN FUNCTIONAL CONNECTIVITY NETWORKS

H. Yang<sup>1,\*</sup>, M. Ortiz-Bouza<sup>1,†</sup>, T. Vu\*, F. Laport\*, V. D. Calhoun\*\*, S. Aviyente<sup>†</sup>, T. Adali\*

\* Dept. of CSEE, University of Maryland, Baltimore County, Baltimore, USA
† Dept. of ECE, Michigan State University, East Lansing, USA

\*\* Tri-institutional Center for Translational Research in Neuroimaging and Data Science (TReNDS),
Georgia State University, Georgia Institute of Technology, and Emory University, Atlanta, USA

## ABSTRACT

Subgroup identification is a fundamental step in precision medicine. Recent research applying data-driven methods such as independent component/vector analysis to multi-subject functional magnetic resonance imaging (fMRI) data has effectively revealed meaningful subgroups. These methods typically focus on single-dimensional information, such as individual functional networks or assuming uniform subgroup structures across networks. Given the complex nature of psychiatric disorders, considering the relationships among subjects across different functional networks can offer valuable insights into diagnostic heterogeneity. We introduce a novel subgroup identification method that leverages multiplex community detection to identify subgroups from multi-subject resting-state fMRI data. The proposed method models subject correlations across functional networks as a multiplex network and identifies common communities across multiple networks and unique communities specific to each functional network. Results from applying the proposed method to 464 psychotic patients show that the identified subgroups exhibit significant group differences on multiple meaningful functional networks as well as the clinical scores, which demonstrate the effectiveness of our method on identifying meaningful subgroups.

*Index Terms*— Subgroup identification, multiplex network, blind source separation, community detection, resting-state fMRI

# 1. INTRODUCTION

Identifying subgroups within a cohort of patients represents a fundamental step in precision medicine, which tailors medical treatments to individuals in different subgroups to minimize medication side-effects [1]. Brain disorders, including neuropsychiatric disorders like bipolar disorder and schizophrenia, often exhibit distinct subtypes [2, 3]. Patients can be categorized into subgroups based on biomarkers associated with specific subtypes. Categorizing neuropsychiatric patients is challenging due to the uncertain etiology of these neuropsychiatric illnesses [4]. Methods that attempt to classify patients based on external observations, such as clinical assessments and cognitive evaluations, have limited success as the connection between subtypes and post hoc descriptions is not well understood.

Subgroup identification methods based on neuroimaging data can rely on objective surrogates such as the structure of functional connectivity networks. Functional magnetic resonance imaging (fMRI) has been widely used to study functional connectivity of the brain, and these networks are identified to be unique as fingerprints [5, 6]. With neuroimaging data, subgroup identification methods by blind source separation algorithms such as independent component analysis (ICA) or independent vector analysis (IVA) have exhibited promising results in identifying meaningful subgroups [7, 8, 9]. Data-driven methods like ICA/IVA offer the key advantage of direct interpretability of the results as functional connectivity networks [10]. However, these subgroup identification methods primarily rely on single-dimensional information, either by focusing on a single functional network or by assuming the same subgroup structure across networks. Given that psychiatric disorders have been associated with abnormalities spanning multiple functional networks [11], considering the relationships among subjects across different functional networks can offer valuable insights for the subgroup identification problem.

Recently, the concept of multiplex networks, which represents multiple modes of interaction across the same set of nodes, has gained attention [12]. A multiplex network is a multilayer network where all layers share the same set of nodes with different topologies. Existing community detection methods for multiplex networks mostly focus on extracting the common community structure across layers. However, in neuroimaging applications, it is important to identify both the shared and unique community structure across a group of functional networks or subjects. While recent research has applied multiplex networks to EEG data to select a subset of edges from the functional connectome as features [13, 14], leveraging multiplex networks to identify subgroups with multi-subject resting-state fMRI data remains relatively unexplored.

In this paper, we propose a subgroup identification method that utilizes multiplex community detection to identify subgroups of subjects from multi-subject resting-state fMRI data. The proposed approach models the covariance matrix of subjects across functional networks as the layers of a multiplex network. Multiplex orthogonal nonnegative matrix tri-Factorization (MX-ONMTF) [15] is then used to identify the common communities across multiple functional networks as well as the unique communities for a certain functional network. We apply the proposed method to 464 psychotic patients, and the results show that the identified subgroups exhibited significant group differences on multiple functional networks, including the anterior prefrontal cortex, dorsal posterior cingulate cortex, visual cortex, etc. These regions have consistently shown abnormalities in various neuropsychiatric disorders. Furthermore, the clinical scores associated with these subgroups also displayed significant group differences, with the observed symptoms closely connected to the functional networks exhibiting group differences.

<sup>&</sup>lt;sup>1</sup> Hanlu Yang and Meiby Ortiz-Bouza contributed equally to this work. This work was supported in part by the grants NIH R01MH118695, NIH R01MH123610, NIH R01AG073949, NSF 2316420, NSF 2006800, and Xunta de Galicia ED481B 2022/012.

The rest of this paper is organized as follows. The proposed method is presented in Section 2. The fMRI data and the corresponding clinical variables are described in Section 3. Results and conclusion are presented in Section 4 and Section 5 separately.

## 2. METHOD

In this section, we describe the different components of the proposed method. We first introduce the definition of source component vector (SCV), based on which the multiplex network is formed. Subsequently, we explain the connection between multiplex community detection and subgroup identification.

## 2.1. Source Component Vector

ICA has been shown to be effective in identifying biomarkers associated with neuropsychiatric disorders [16, 17]. Constrained EBM (c-EBM), a constrained ICA algorithm based on minimizing the source entropy bound, provides a more flexible model match without imposing orthogonality constraints on the demixing matrix. C-EBM leverages a set of spatial maps as constraints to establish connections across datasets, serving as a foundation for subgroup identification. Recent research has demonstrated the successful application of c-EBM in addressing the subgroup identification problem [18]. In this work, c-EBM, is applied to K subjects individually. The ICA model for the  $k^{\rm th}$  subject can be written as

$$\mathbf{x}^{[k]}(v) = \mathbf{A}^{[k]}\mathbf{s}^{[k]}(v), \ 1 \le v \le V.$$
 (1)

where  $\mathbf{x}^{[k]}(v) = [x_1^{[k]}(v), \dots, x_L^{[k]}(v)]^{\top}$  is an observation vector at sample index v (superscript  $\top$  represents transpose);  $\mathbf{A}^{[k]} \in \mathbb{R}^{L \times L}$  represents an unknown invertible mixing matrix, and  $\mathbf{s}^{[k]}(v) = [s_1^{[k]}(v), \dots, s_L^{[k]}(v)]^{\top}$  are L statistically independent, zero mean, and unit variance latent sources. With the provided prior information serving as constraints, c-EBM estimates the latent sources by estimating a demixing matrix  $\mathbf{W}^{[k]} \in \mathbb{R}^{L \times L}$  such that the estimates  $\mathbf{y}^{[k]}(v) = [y_1^{[k]}(v), \dots, y_L^{[k]}(v)]^{\top}$ , where  $\mathbf{y}^{[k]}(v) = \mathbf{W}^{[k]}\mathbf{x}^{[k]}(v)$ , are maximally independent. The constraints serve as a foundation for subgroup identification by establishing connections across the subjects and aligning subject-wise components from separate ICA analyses. We define the  $l^{th}$  source component vector (SCV) as  $\mathbf{s}_l(v) = [\mathbf{s}_l^{[1]}(v), \dots, \mathbf{s}_l^{[K]}(v)]^{\top} \in \mathbb{R}^K$ , which is the concatenation of the  $l^{th}$  source from each of the K datasets. Accordingly, the estimate of the  $l^{th}$  SCV is denoted by  $\mathbf{y}_l(v) = [y_l^{[1]}(v), \dots, y_l^{[K]}(v)]^{\top}$ . The illustration of SCV can be found in Fig. 1. In the context of fMRI data, the  $l^{th}$  SCV summarizes the spatial activation pattern of the  $l^{th}$  component, such as default mode network, across all K subjects. For a total of V samples, the estimated sample covariance matrix of the  $l^{th}$  SCV is given by  $\hat{\mathbf{C}}_l = \frac{1}{V-1}\mathbf{Y}_l\mathbf{Y}_l^{\top}$ , where  $\mathbf{Y}_l = [\mathbf{y}_l^{[1]}, \dots, \mathbf{y}_l^{[K]}]^{\top} \in \mathbb{R}^{K \times V}$  and  $\mathbf{y}_l^{[K]} = [\mathbf{y}_l^{[k]}(1), \dots, \mathbf{y}_l^{[K]}(V)] \in \mathbb{R}^{V}$  is a row vector of the estimation for the  $k^{th}$  subjects for a given functional network.

# 2.2. Multiplex Community Detection

Given the sample covariance matrix of the  $l^{\text{th}}$  SCV,  $\hat{\mathbf{C}}_l$ , with  $l \in \{1,2,\ldots,L\}$  corresponding to the different SCVs, we can construct a multiplex graph  $\mathcal{G}_l = (\mathcal{V}, E_l, |\hat{\mathbf{C}}_l|)$ , where  $\mathcal{V}$  denotes the set of K nodes (subjects),  $E_l$  the set of edges, and  $|\hat{\mathbf{C}}_l| \in \mathbb{R}^{K \times K}$  represents the adjacency matrix for layer l. The illustration of forming the multiplex network can be found in Fig. 1. In this paper, MX-ONMTF [15], which models each layer's adjacency matrix as the sum of low-rank representations of common and private communities, is used to

identify the community structure. A common community refers to a collection of nodes that are assigned to the same community in more than a single layer, whereas a private community is defined as any community that is not common across at least two layers.

For a multiplex network with L layers that is formed from covariance matrices,  $\hat{\mathbf{C}}_l \in \mathbb{R}^{K \times K}, l \in \{1, 2, \dots, L\}$ , the objective function in [15] is reformulated as

$$\underset{\mathbf{H} \geq 0, \mathbf{H}_{l} \geq 0, \mathbf{M}_{l} \geq 0, \mathbf{G}_{l} \geq 0}{\operatorname{argmin}} \sum_{l=1}^{L} |||\hat{\mathbf{C}}_{l}| - \mathbf{H}\mathbf{M}_{l}\mathbf{H}^{\top} - \mathbf{H}_{l}\mathbf{G}_{l}\mathbf{H}_{l}^{\top}||_{F}^{2}$$
s.t  $\mathbf{H}^{\top}\mathbf{H} = \mathbf{I}, \mathbf{H}_{l}^{\top}\mathbf{H}_{l} = \mathbf{I}, \text{with } l \in \{1, 2, \dots, L\},$ 

where  $\mathbf{H} \in \mathbb{R}^{K \times P_c}$  and  $\mathbf{H}_l \in \mathbb{R}^{K \times P_l}$ , are the community membership matrices corresponding to the common and private communities, respectively, and  $\mathbf{M}_l \in \mathbb{R}^{P_c \times P_c}$  and  $\mathbf{G}_l \in \mathbb{R}^{P_l \times P_l}$  are diagonal matrices that capture the inter-community interactions with  $P_c$  and  $P_l$  corresponding to the total number of common communities, and the number of private communities in layer l, respectively.

The optimization in (2) can be solved using a multiplicative update algorithm as given in [15].  $P_c$  and  $P_l$  are determined following the eigengap and hierarchical clustering-based method proposed in [15]. First, the total number of communities per layer is determined using the Eigengap rule [19], followed by applying orthogonal nonnegative matrix tri-factorization to each layer. This results in embedding matrices representing the nodes' community affiliations for each layer. Subsequently, an agglomerative hierarchical clustering algorithm is applied to these matrices to determine  $P_c$  and  $P_l$ . Since  $\mathbf{H} \in \mathbb{R}^{K \times P_c}$  is the community membership matrix corresponding to all of the common communities, to determine whether a node from a particular layer belongs to any of the common communities, H needs to go through post-processing. In this paper, we propose a flexible community assignment criterion. Once the subset of layers that are assigned to each common community is identified, a node iis assigned to a common community j if the value of common community membership,  $\mathbf{H}(i,j)$ , is greater than the majority (i.e., 80%) of the private community membership values,  $\mathbf{H}_{l}(i, j)$ , for all layers l where community j is present. This ensures that while the common communities contain mostly the same set of nodes (subjects) across layers (functional networks), there is still room for some variation of the common community structure. We evaluated thresholds ranging from 100% to 50%. The standard deviation of the number of nodes assigned to common communities showed a significant increase when the threshold fell below 80%. Consequently, we chose 80% as the appropriate threshold for the current dataset. The nodes that are not assigned to any common community are assigned to private communities in each layer l by identifying the column of  $\mathbf{H}_l$ with the highest value for their corresponding rows. We summarize this procedure in Algorithm 1.

# 3. RESTING-STATE FMRI DATA

The resting-state fMRI datasets and the corresponding clinical scores are collected from the Bipolar-Schizophrenia Network on Intermediate Phenotypes (B-SNIP) study [20, 21]. All subjects underwent a single 5-minute run of resting-state fMRI on a 3-T scanner. Subjects were instructed to keep their eyes open, focus on a crosshair displayed on a monitor, and remain still during the entire scan.

We removed the first three time points and performed head motion correction followed by slice-timing correction. The corrected fMRI data were then warped into standard Montreal Neurological Institute (MNI) space and resampled to  $3\times3\times3$  mm³ isotropic voxels. The resampled fMRI data were further smoothed using a Gaussian kernel with a full width at half maximum (FWHM) equal

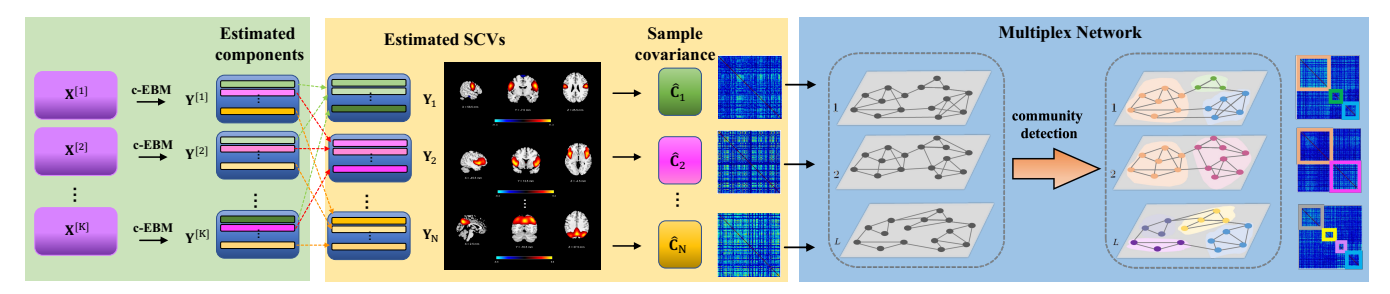


Fig. 1. Flowchart of the proposed method. Subject-wise c-EBM is applied to individual datasets. The  $l^{th}$  SCV can be formed by concatenating the  $l^{th}$  component from all estimates. The sample covariance matrix of  $l^{th}$  SCV,  $\hat{\mathbf{C}}_l$ , provides the correlation information among K subjects for a given functional network. Each  $\hat{\mathbf{C}}_l$  can then be transformed into a weighted undirected graph, where subjects are represented as nodes, and the absolute values of the correlation values across subjects for a particular functional network serve as edge weights. Subsequently, a multiplex network-based community detection algorithm is applied to reveal the community structures.

## Algorithm 1 Assigning community labels

**Input:** Community membership matrices  $\mathbf{H}$  and  $\mathbf{H}_l$ , the number of common  $P_c$ , and private communities  $P_l$ ,  $l \in \{1, 2, ..., L\}$ 

**Output:** Community labels  $idx_l$  for each layer.

```
1: for each common community p_c \in \{1, 2, \dots, P_c\} do
          Identify the set of layers where p_c is present, l_c.
 2:
 3:
          for each layer l in l_c do
              for each node i do
 4:
                  j^* \leftarrow \operatorname{argmax}_{j} \mathbf{H}(i, j)
m = |\mathbf{H}(i, j^*) > [\mathbf{H}_{l_c}(i, :)]|
if m > 0.8 \sum_{l \in l_c} P_l then
i dx_l(i) \leftarrow j^*
 5:
 6:
 7:
 8:
                  else
 9.
                       idx_l(i) \leftarrow (argmax_i \mathbf{H}_l(i,j)) + P_c + \sum_{n=1}^{l-1} P_n
10:
11:
12:
              end for
13:
          end for
14: end for
15: for each layer l do
          find n_p = \text{find}(idx_l == 0)
16:
          for each node i in n_p do
17:
              idx_l(i) \leftarrow (\operatorname{argmax}_i \mathbf{H}_l(i,j)) + P_c + \sum_{n=1}^{l-1} P_n
18:
19:
          end for
20: end for
```

to 6 mm. We use 464 individuals diagnosed with psychotic disorders in this study. The spatial constraints for c-EBM are derived from the fSIG pipeline, which comprises 49 resting-state networks (RSNs) including auditory (AUD: 1 RSN), sensorimotor (MOT: 8 RSNs), visual (VIS: 10 RSNs), default-mode (DMN: 11 RSNs), attentional (ATTN: 8 RSNs), frontal (FRONT: 8 RSNs), cerebellar (CB: 2 RSNs), and basal ganglia (BG: 1 RSN) networks [9].

The Positive and Negative Syndrome Scale (PANSS) [22] are collected from the same group of individuals. The PANSS scores encompass 30 disparate symptoms observed in psychotic patients and are scored on a scale ranging from 1 to 7. These scores consistently capture three symptom dimensions: positive, negative, and general [23]. PANSS has been applied to quantify variations of functional networks across individuals with psychotic conditions [24, 25]. In cases where clinical scores are missing for certain subjects, the values are padded with the mean of that specific test or subtest, calculated from all subjects with available test data.

## 4. RESULTS

We applied the MX-ONMTF algorithm to a multiplex network with L=49 and K=464 corresponding to the aforementioned 49 resting-state networks and 464 psychotic patients. The determined number of communities is 7 common communities across different subsets of networks and a total of 105 private communities.

A two-sample t-test was employed to analyze the activation value at each voxel of the spatial maps across the subjects within each subgroup to determine whether the spatial activation patterns of RSNs show significant group differences across subgroups. False discovery rate (FDR) correction [26] is included in all comparisons. The first common community is identified across 11 functional networks and exhibits significant group differences from the rest of the subjects in multiple meaningful functional connectivity networks. In addition, we observe a connection between the neuro-activity t-maps and clinical scores. In Fig. 2(a), layer 34 (ATTN), we observe significant group differences (p = 0.00917) in the anterior prefrontal cortex (antPFC, BA 10), dorsolateral prefrontal cortex (dlPFC, BA 9), middle occipital gyrus (BA 37), and angular gyrus (BA 39). In Fig. 2(b), layer 37 (ATTN), we observe significant group differences (p = 0.00256) in the dorsal posterior cingulate cortex (dIPCC BA 31), anterior insula (AI, BA 13) ares, where dlPCC is a key node in the default mode network and AI is part of salience network. The anomalous connectivity of these two could be associated with a greater risk for psychiatric disorders [27, 28].

These differences in the aforementioned neuro-activity t-maps are aligned with findings in neuroimaging research and the group differences observed in PANSS scores. In Fig. 2(c), we summarize the dominant and absent symptoms of the identified common community. The dominant symptoms of a community are characterized by median values greater than 2 or the median value is 2 for one community while it is 1 (which means absent) for the other community. For instance, the antPFC regions, associated with cognitive functions like abstraction [29] and relational reasoning [30], show reduced activation in subjects from the common community 4, potentially contributing to symptoms such as difficulties in abstract thinking. Similarly, the decreased local connectivity in the dIPFC, known for its role in higher cognitive functions like working memory and inhibiting inappropriate responses [31], might reflect deficiencies in thought suppression processes. Furthermore, the abnormal activation observed in the middle occipital gyrus and angular gyrus may be linked to severe symptoms such as anxiety and grandiosity [32, 33, 34]. Research from [35] indicates that altered connectivity in the PCC area is associated with both positive and negative symp-

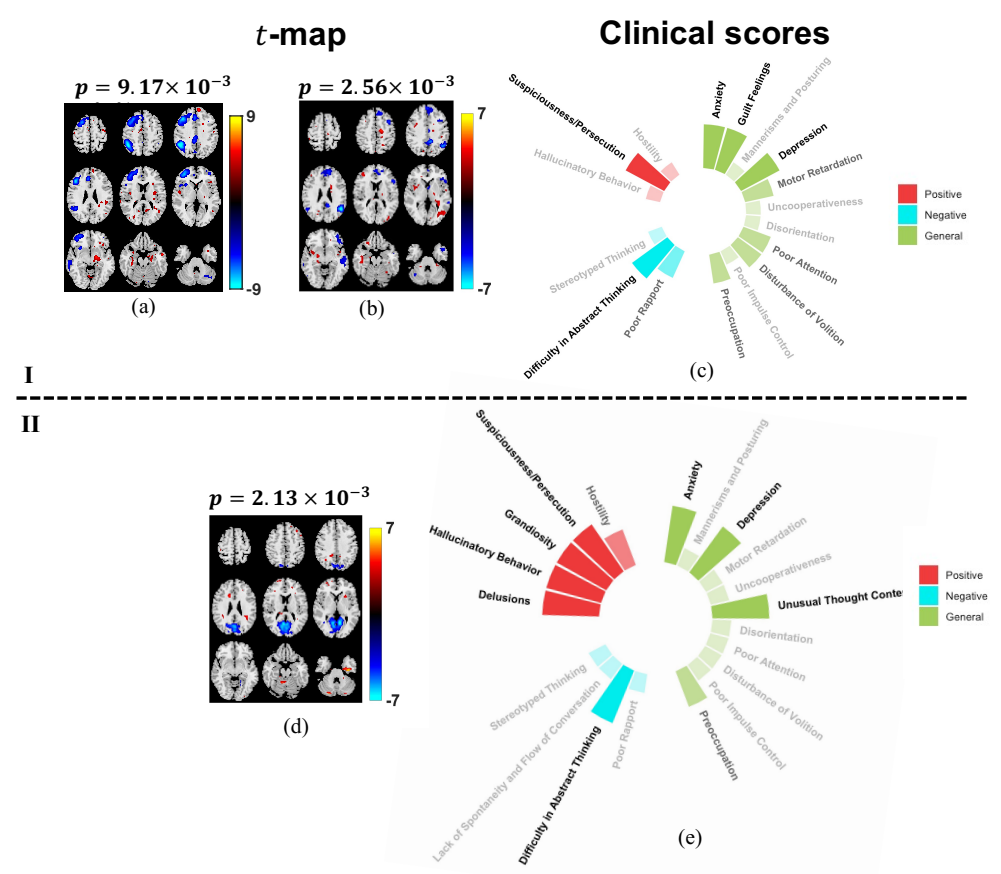


Fig. 2. The identified subgroups exhibit notable disparities in both neuro-activity maps (t-maps) and clinical scores. The distinctions in spatial activation patterns between the first common community and the rest of the subjects are quantified via a two-sample t-test with FDR (< 0.05). For the first identified subgroup, which is presented in I, the group differences shown in neuro-activity maps are displayed in (a) and (b), and the corresponding differences in clinical scores can be observed in (c). Similarly, for the second identified subgroup, the corresponding results are displayed in (d) and (e).

toms in schizophrenia, which aligns with the more severe positive symptoms observed in the common communities.

Another common community identified by the proposed method (across 21 functional networks) also exhibits significant group differences in meaningful brain areas. For example, in Fig. 2(d), layer 14 (VIS), we observe significant group differences (p = 0.00213) in the secondary visual cortex (BA 18), and superior parietal lobule (BA 7). Studies highlight that the visual cortex has multisensory functions beyond mere visual processing, which can directly affect subjects' behavior and perception. Increased visual perceptual abnormalities (VPAs) are reported to be associated with multiple clinical features, including depressive and bizarre behavior symptoms in psychotic disorders [36]. The superior parietal lobule has close links with the occipital lobe and is involved in functions of attention and visuospatial perception, including the representation and manipulation of objects [37]. The clinical scores are aligned with the aforementioned neuro-activity t-maps. For example, in Fig. 2(e), the dominant symptoms observed from the common community 5 include poor attention, depression, and persecution may be caused by the abnormal connectivity observed in the visual cortex and superior parietal lobule.

## 5. CONCLUSION

Identifying subgroups from a cohort of patients is a challenging problem and has recently started to receive attention. In this work,

a novel subgroup identification method based on multiplex community detection is introduced. The proposed method considers multi-dimensional information from functional connectivity networks for subgroup identification. In contrast to recent approaches that only rely on one-dimensional information, our method characterizes subject correlations across multiple functional networks as a multiplex network, which uncovers both shared communities across multiple networks and unique communities specific to each functional network. Results from real fMRI data show that the identified subgroups exhibit significant group differences on multiple meaningful functional networks as well as the clinical scores. The concordance between the identified subgroups and the observed differences in clinical scores relating to symptoms demonstrates the effectiveness of our method in identifying meaningful subgroups.

Currently, our method is only applied to datasets comprising psychiatric patients. To further validate its generalizability and robustness, future work will involve extending its application to a larger and more diverse dataset. Given the familial aggregation of certain mental disorders, like schizophrenia, it is pertinent to explore datasets encompassing healthy relatives of patients. This exploration aims to investigate whether analogous subgroup patterns emerge among the relatives, which provides valuable insights into the hereditary aspects of these disorders.

## 6. REFERENCES

- N. R. Council et al., "Toward precision medicine: building a knowledge network for biomedical research and a new taxonomy of disease," 2011.
- [2] J. Biederman, E. Mick, S. V. Faraone, T. Spencer, T. E. Wilens, and J. Wozniak, "Pediatric mania: a developmental subtype of bipolar disorder?," *Biol. Psychiatry*, vol. 48, no. 6, pp. 458–466, 2000.
- [3] M. T. Tsuang, M. J. Lyons, and S. V. Faraone, "Heterogeneity of schizophrenia," BJPsych, vol. 156, no. 1, pp. 17–26, 1990.
- [4] D. B. Dwyer, C. Cabral, L. Kambeitz-Ilankovic, R. Sanfelici, J. Kambeitz, V. Calhoun, P. Falkai, C. Pantelis, E. Meisenzahl, and N. Koutsouleris, "Brain subtyping enhances the neuroanatomical discrimination of schizophrenia," *Schizophr. Bull.*, vol. 44, no. 5, pp. 1060–1069, 2018.
- [5] E. S. Finn, X. Shen, D. Scheinost, M. D. Rosenberg, J. Huang, M. M. Chun, X. Papademetris, and R. T. Constable, "Functional connectome fingerprinting: identifying individuals using patterns of brain connectivity," *Nat. Neurosci.*, vol. 18, no. 11, pp. 1664–1671, 2015.
- [6] V. D. Calhoun, T. Eichele, and G. Pearlson, "Functional brain networks in schizophrenia: a review," Front. Hum. Neurosci., vol. 3, pp. 17, 2009.
- [7] Q. Long, S. Bhinge, V. D. Calhoun, and T. Adali, "Independent vector analysis for common subspace analysis: Application to multi-subject fMRI data yields meaningful subgroups of schizophrenia," *NeuroImage*, vol. 216, pp. 116872, 2020.
- [8] H. Yang, M. Akhonda, F. Ghayem, Q. Long, V. Calhoun, and T. Adali, "Independent vector analysis based subgroup identification from multisubject fMRI data," in *Proc. IEEE Int. Conf. Acoust. Speech Signal Process.* IEEE, 2022, pp. 1471–1475.
- [9] H. Yang, T. Vu, Q. Long, V. Calhoun, and T. Adali, "Identification of homogeneous subgroups from resting-state fmri data," *Sensors*, vol. 23, no. 6, pp. 3264, 2023.
- [10] T. Adali, M. Anderson, and G.-S. Fu, "Diversity in independent component and vector analyses: Identifiability, algorithms, and applications in medical imaging," *IEEE Signal Process. Mag*, vol. 31, no. 3, pp. 18–33, 2014
- [11] V. Menon, "Large-scale brain networks and psychopathology: a unifying triple network model," *Trends Cogn Sci.*, vol. 15, no. 10, pp. 483–506, 2011.
- [12] M. Vaiana and S. F. Muldoon, "Multilayer brain networks," J. Nonlinear Sci., vol. 30, no. 5, pp. 2147–2169, 2020.
- [13] B. Osterkamp, M. Ortiz-Bouza, and S. Aviyente, "Variability of functional connectomes through community structure," in 2023 IEEE Int. Conf. Acoust. Speech Signal Process. Workshops. IEEE, 2023, pp. 1–5.
- [14] G. Frusque, J. Jung, P. Borgnat, and P. Gonçalves, "Multiplex network inference with sparse tensor decomposition for functional connectivity," *IEEE transactions on Signal and Information Processing over Networks*, vol. 6, pp. 316–328, 2020.
- [15] M. Ortiz-Bouza and S. Aviyente, "Community detection in multiplex networks based on orthogonal nonnegative matrix tri-factorization," *IEEE Access*, vol. 12, pp. 6423–6436, 2024.
- [16] S. Bhinge, Q. Long, V. D. Calhoun, and T. Adali, "Spatial dynamic functional connectivity analysis identifies distinctive biomarkers in schizophrenia," *Front. Neurosci.*, vol. 13, pp. 1006, 2019.
- [17] V. D. Calhoun and T. Adali, "Multisubject independent component analysis of fMRI: a decade of intrinsic networks, default mode, and neurodiagnostic discovery," *IEEE Rev. Biomed. Eng.*, vol. 5, pp. 60– 73, 2012.
- [18] H. Yang, F. Ghayem, B. Gabrielson, M. A. B. S. Akhonda, V. D. Calhoun, and T. Adali, "Constrained independent component analysis based on entropy bound minimization for subgroup identification from multi-subject fMRI data," in *Proc. IEEE Int. Conf. Acoust. Speech Signal Process.* IEEE, 2023, pp. 1–5.
- [19] F. Liu, D. Choi, L. Xie, and K. Roeder, "Global spectral clustering in dynamic networks," *Proceedings of the National Academy of Sciences*, vol. 115, no. 5, pp. 927–932, 2018.

- [20] C. A. Tamminga, E. I. Ivleva, M. S. Keshavan, G. D. Pearlson, B. A. Clementz, B. Witte, D. W. Morris, J. Bishop, G. K. Thaker, and J. A. Sweeney, "Clinical phenotypes of psychosis in the bipolar-schizophrenia network on intermediate phenotypes (b-snip)," Am. J. Psychiatry, vol. 170, no. 11, pp. 1263–1274, 2013.
- [21] C. A. Tamminga, G. Pearlson, M. Keshavan, J. Sweeney, B. Clementz, and G. Thaker, "Bipolar and schizophrenia network for intermediate phenotypes: outcomes across the psychosis continuum," *Schizophr. Bull.*, vol. 40, no. Suppl.2, pp. S131–S137, 2014.
- [22] S. R. Kay, A. Fiszbein, and L. A. Opler, "The positive and negative syndrome scale (panss) for schizophrenia," *Schizophr. Bull.*, vol. 13, no. 2, pp. 261–276, 1987.
- [23] C. Lancon, P. Auquier, G. Nayt, and G. Reine, "Stability of the five-factor structure of the positive and negative syndrome scale (panss)," *Schizophr. Res.*, vol. 42, no. 3, pp. 231–239, 2000.
- [24] W. Yan, M. Zhao, Z. Fu, G. D. Pearlson, J. Sui, and V. D. Calhoun, "Mapping relationships among schizophrenia, bipolar and schizoaffective disorders: a deep classification and clustering framework using fmri time series," *Schizophr. Res.*, vol. 245, pp. 141–150, 2022.
- [25] S. A. Meda, A. Gill, M. C. Stevens, R. P. Lorenzoni, D. C. Glahn, V. D. Calhoun, J. A. Sweeney, C. A. Tamminga, M. S. Keshavan, G. Thaker, et al., "Differences in resting-state fmri functional network connectivity between schizophrenia and psychotic bipolar probands and their unaffected first-degree relatives," *Biol. Psychiatry*, vol. 71, no. 10, pp. 881, 2012.
- [26] Y. Benjamini and D. Yekutieli, "False discovery rate-adjusted multiple confidence intervals for selected parameters," *J. Acoust. Soc. Am.*, vol. 100, no. 469, pp. 71–81, 2005.
- [27] L. Palaniyappan, T. P. White, and P. F. Liddle, "The concept of salience network dysfunction in schizophrenia: from neuroimaging observations to therapeutic opportunities," *Curr. Top. Med. Chem.*, vol. 12, no. 21, pp. 2324–2338, 2012.
- [28] S. Whitfield-Gabrieli, H. W. Thermenos, S. Milanovic, M. T. Tsuang, S. V. Faraone, R. W. McCarley, M. E. Shenton, A. I. Green, A. Nieto-Castanon, P. LaViolette, et al., "Hyperactivity and hyperconnectivity of the default network in schizophrenia and in first-degree relatives of persons with schizophrenia," *Proc. Natl. Acad. Sci.*, vol. 106, no. 4, pp. 1279–1284, 2009.
- [29] K. Christoff, K. Keramatian, A. M. Gordon, R. Smith, and B. M\u00e4dler, "Prefrontal organization of cognitive control according to levels of abstraction," *Brain Res.*, vol. 1286, pp. 94–105, 2009.
- [30] K. Christoff, V. Prabhakaran, J. Dorfman, Z. Zhao, J. K. Kroger, K. J. Holyoak, and J. D. Gabrieli, "Rostrolateral prefrontal cortex involvement in relational integration during reasoning," *Neuroimage*, vol. 14, no. 5, pp. 1136–1149, 2001.
- [31] I. Hertrich, S. Dietrich, C. Blum, and H. Ackermann, "The role of the dorsolateral prefrontal cortex for speech and language processing," *Front. Hum. Neurosci.*, vol. 15, pp. 645209, 2021.
- [32] S.-W. Xue, Q. Yu, Y. Guo, D. Song, and Z. Wang, "Resting-state brain entropy in schizophrenia," *Compr. Psychiatry*, vol. 89, pp. 16–21, 2019.
- [33] C. Qiu, W. Liao, J. Ding, Y. Feng, C. Zhu, X. Nie, W. Zhang, H. Chen, and Q. Gong, "Regional homogeneity changes in social anxiety disorder: a resting-state fmri study," *Psychiatry Res. Neuroimaging*, vol. 194, no. 1, pp. 47–53, 2011.
- [34] U. Frith and C. D. Frith, "Development and neurophysiology of mentalizing," *Philos. Trans. R. Soc. Lond., B, Biol. Sci.*, vol. 358, no. 1431, pp. 459–473, 2003.
- [35] A. Rotarska-Jagiela, V. van de Ven, V. Oertel-Knöchel, P. J. Uhlhaas, K. Vogeley, and D. E. Linden, "Resting-state functional network correlates of psychotic symptoms in schizophrenia," *Schizophr. Res.*, vol. 117, no. 1, pp. 21–30, 2010.
- [36] B. P. Keane, L. N. Cruz, D. Paterno, and S. M. Silverstein, "Self-reported visual perceptual abnormalities are strongly associated with core clinical features in psychotic disorders," *Front. Psychiatry*, vol. 9, pp. 69, 2018.
- [37] P. Johns, Functional neuroanatomy, Elsevier, 2014.